2 (2022) 100012

Contents lists available at ScienceDirect

IPEM-Translation

journal homepage: www.elsevier.com/locate/ipemt

Full Length Article

Comparison of SNR Assessment Techniques for Routine Multi-Element RF Coil QC Testing

James Harkin [*,a], Cameron Ingham [b]

[a] The Christie NHS Foundation Trust, Wilmslow Rd, Manchester M20 4BX
[b] University Hospitals Dorset NHS Foundation Trust, Longfleet Rd, Poole, BH15 2JB

ARTICLE INFO

Keywords:
MRI
QC
Quality Control
QA
Quality assurance
SNR
Signal-to-Noise Ratio
RF Coil
Medical Physics

ABSTRACT

In the UK, the Institute of Physics and Engineering in Medicine (IPEM) provides guidance to Medical Physics departments on appropriate Quality Control (QC) tests to evaluate MRI scanners used in routine clinical practice. The method recommended for the rigorous annual assessment of the SNR produced by RF coils uses a sequence and regions of interest (ROIs) recommended by IPEM, and calculates SNR through a subtraction calculation (*IPEM recommended Method*). This method was compared to alternative methods proposed by NessAiver at the 2019 American Association of Physicists in Medicine meeting in their talk on RF coil testing. Comparisons were completed for sequences and regions of interest (ROIs) recommended by IPEM and NessAiver. Testing was performed at 1.5 T using the scanner's integrated body coil and at 3.0 T using a peripheral Head/Neck coil. Calculation of SNR using the mean of the background noise, assessed using the NessAiver recommended sequence and ROIs (*NessAiver Noise-Average Method*), typically offered the lowest variability in SNR results. Additionally, the SNR results produced by the *IPEM Recommended Method* were less repeatable than those from the *NessAiver Noise-Average Method* ($p<0.001$). Furthermore, the significance level to which a simulated reduction in SNR could be detected using the *IPEM Recommended Method* ($p<0.001$) was less than with the *NessAiver Noise-Average Method* ($p\geq0.0031$). Finally, when comparing the test duration of each method, use of the *NessAiver Noise-Average Method* results in a 90% reduction in acquisition time per SNR result, when compared to the *IPEM Recommended Method*.

1. Introduction

For the majority of MRI in clinical practice, the transmitted Radio Frequency (RF) pulse is produced by a birdcage or transverse electromagnetic (TEM) coil, such as the integrated body coil, which is capable of producing a sufficiently homogeneous transmit field. In order to increase the received signal from the region of interest (ROI), peripheral RF coils are employed. These coils are generally receive only; consisting of multiple, surface, receive coil elements, which possess a high sensitivity, but low penetration depth. This means that, for routine clinical assessments, multiple peripheral RF coils are required, optimised for different anatomies, designed to place the surface coils close to the anatomy of interest.

Using multiple small surface coils also allows some information about the spatial origin of the MR signal to be determined, and this information can be used to reduce acquisition times through parallel imaging methods. In recent years the number of surface coils used has increased, with Siemens now offering a 64 channel head coil commercially[1]. With so many elements in coils, it is possible for a multi element failure to go unnoticed in routine *in vivo* imaging[2]. It is therefore important that the responses from individual coil elements are interrogated, to confirm the RF coils are functioning as expected and to determine any needs for corrective actions such that equipment meets the expected standards.

1.1. Current RF Coil Testing Guidance

In the UK, the Institute of Physics and Engineering in Medicine

Abbreviations: BW, Bandwidth; CE, Combined Element; IE, Individual Element; IPEM, Institute of Physics and Engineering in Medicine; MRI, Magnetic Resonance Imaging; NEMA, National Electrical Manufacturers Association; PE, Phase Encodings; QC, Quality Control; RF, Radio Frequency; ROI, Region of Interest; SD, Standard Deviation; SNR, Signal-to-Noise Ratio; SoS, Sum of Squares; SW, Slice Width; TE, Echo Time; TEM, Transverse Electromagnetic; TR, Repetition Time.

* Corresponding author.
E-mail addresses: jameswharkin@gmail.com (J. Harkin), cameron.ingham2@gmail.com (C. Ingham).

https://doi.org/10.1016/j.ipemt.2022.100012
Received 24 June 2022; Received in revised form 26 October 2022; Accepted 8 November 2022
Available online 12 November 2022

(IPEM) provides guidance to Medical Physics departments on appropriate Quality Control (QC) tests to evaluate MRI scanners used in routine clinical practice. This guidance is outlined in IPEM Report 112 [3]. The most common way of assessing the performance of RF coils is through assessment of the signal to noise ratio (SNR) from the images they produce of uniform phantoms, and this will be the focus of this study. With regards to routine SNR QC, current IPEM guidelines recommend the following:

- Daily/Weekly SNR tests, using the "background" SNR analysis method[3]. Testing should cycle through the available coils, with a particular focus on the more regularly used coils. Results should be compared to those gathered at acceptance.
- Annually, all coils should be tested, especially those not regularly tested in daily/weekly QC. Testing should be performed using the NEMA subtraction SNR analysis method[4], and results should be compared to those gathered at acceptance.

1.2. Calculating SNR

The most accurate method of calculating SNR from MR image data is to calculate the SNR of each pixel individually using Equation 1. This method requires a large number of images to be acquired to form a representative average. Calculated across these acquisitions, $\mu(x,y)$ is the average signal of the pixel and $\sigma(x,y)$ is the standard deviation (SD) of the pixel. This method is limited in the fact that MR acquisitions take a long time and calculation of SNR pixel by pixel is a laborious process. It is consequently not practical in a clinical setting where scanner time is in high demand.

$$SNR(x,y) = \frac{\mu(x,y)}{\sigma(x,y)} \tag{1}$$

To reduce the time required to perform SNR QC, IPEM recommends the "Subtraction" or "Background SD" SNR calculation methods. These rely on different methods of estimating the noise in an image.

1.2.1. Subtraction Calculation

For the subtraction SNR calculation method, two magnitude images are acquired, from which a further image is generated by subtracting one of the acquired images from the other. The noise in signal-producing regions of the subtracted image is expected to follow a Gaussian distribution (with a variance twice that of an single image). SNR is calculated through Equation 2, where μ_0 is the mean pixel intensity in one of the phantom images and σ_{sub} is the SD in the subtracted image. NEMA recommends calculating μ_0 and σ_{sub} across a single large ROI, enclosing at least 75% of the area of the image of the signal-producing volume of the phantom, and avoiding edge effects (A in Figure) [4].

$$SNR_{sub} = \frac{\sqrt{2}\mu_0}{\sigma_{sub}} \tag{2}$$

1.2.2. Background SD Calculation

In contrast to the previous methods described, to perform a background SD calculation, only one magnitude image is required. The signal in the background of a single element coil image follows a Rayleigh distribution, meaning the SD of the signal in the image background is theoretically proportional to the noise[5]. This allows SNR to be calculated through Equation 3. A correction factor is employed in the calculation to correct for the non-Gaussian noise distribution (f_σ). For single element images this correction factor is equal to 0.66[5]. For multi-element images, Constantinides et al.[6] have derived correction factors for sum of squares (SoS) combinations of individual element images. IPEM recommends calculating σ_{air} (the SD in the image background) by averaging across several ROIs outside the phantom region. The example ROIs[7] given in IPEM Report 112 for background noise (reproduced as B in Figure) are not fixed. It is noted that they "could be any shape as long as they encompass a sufficient area to obtain a good estimation of the noise distribution and avoid regions of image artefacts"[3].

$$SNR_{B\sigma} = \frac{f_\sigma \mu_0}{\sigma_{air}} \tag{3}$$

1.2.3. Background Mean Calculation

In their presentation at the 2019 American Association of Physicists in Medicine Meeting, and their subsequent report on the topic[8], NessAiver suggests an alternative equation for calculating SNR (Equation 4), with the noise in the image estimated using μ_{air}, equal to the average intensity of the pixels in the background of the magnitude image. To correct for the non-Gaussian nature of the noise distribution, a different correction factor (f_μ) is required, equal to 1.25 for single element images. Constantinides et al.[6] have also derived correction factors for sum of squares (SoS) combinations of individual element images.

$$SNR_{B\mu} = \frac{f_\mu \mu_0}{\mu_{air}} \tag{4}$$

NessAiver also suggests that different ROIs should be used compared to those given by IPEM (Figure); ROIs should cover as much of the phantom/air regions as possible, while avoiding edge effects.

1.3. Image Acquisition

For assessments of SNR, current IPEM guidelines recommend acquiring a Spin Echo (SE) image using the sequence parameters defined in Table 1, this generates a high SNR T2-weighted image. In contrast, NessAiver suggests using a lower SNR SE sequence (see Table 1). The motivation for acquiring a lower SNR sequence, considering the background mean calculation method, is that the intensity of the in-air pixels will be higher than the IPEM recommended sequence, and therefore estimations of the noise should theoretically improve. However, it has been noted that the use of exceptionally low SNR images may not be optimal when using a fixed-point formula for SNR[10]. It is also known that images produced in MRI have integer pixel values, as such, with a very high SNR image, a large proportion of the air pixels are often truncated (or rounded) to a limited number of values (i.e. 0, 1 and 2), making it very difficult to get a good estimate of the true variance of the Rayleigh distribution[8]. Furthermore, high SNR images will lead to more pronounced Gibbs-ringing, which may dominate "true" noise around the phantom periphery.

In both cases, it is vital that images are acquired in a consistent manner, both in terms of acquisition parameters and positioning, in order to ensure consistent SNR results. Greater repeatability allows for tighter action levels to be defined and consequently coil defects are more likely to be discovered.

It is also important to acquire images with as little post processing as possible and the application of filters must be carefully controlled[2]. In particular, geometric distortion filters should not be applied, as they are known to result in local resampling of both the signal and noise regions,

Table 1
Recommended sequence acquisition parameters by IPEM[3] (a.) and NessAiver [8] (b.), with regards to: repetition time (TR), echo time (TE), slice width (SW) and phase encodings (PE).

	Sequence	TR (ms)	TE (ms)	SW (mm)	PE	Duration
a.	**IPEM**	1000	30	5	256	4 min. 15 sec.
b.	**NessAiver**	200	20	~1.2 (smallest possible)	256	51 sec.

which will affect the distribution of pixel intensities and hence the variance[8]. Similarly, the application of acquisition techniques for multi-channel surface coil arrays, such as parallel imaging and certain reconstruction filters, can influence the statistical distribution of image noise; leading to inaccurate estimations of the true local noise level for methods assessing the image background[11]. Since they are of benefit to in vivo imaging, the removal of filters may not be straightforward for all scanner models and may require more information than is provided in the manuals[8]. Combined element (CE) images should also be generated using a SoS combination of the individual element (IE) images, because scanner adaptive reconstruction algorithms can significantly reduce background noise levels[12].

Considering the parameters outlined in Table 1, the sequence recommended by NessAiver takes 20% of the time to acquire compared to the IPEM recommended sequence. Additionally, if SNR can be accurately characterised through analysis of the noise from the image background, only one acquisition is required. This means that switching from the IPEM recommended sequence and SNR_{sub} (Equation 2), to the NessAiver recommended sequence and assessment using $SNR_{B\sigma}$ (Equation 3) or $SNR_{B\mu}$ (Equation 4) could lead to a 90% reduction in acquisition time for the SNR analysis of each RF coil.

2. Methods

Testing was performed, comparing different SNR evaluation methods to the method recommended by IPEM for rigorous annual RF coil SNR QC testing (*IPEM recommended Method*).

Individual coil element images were acquired using the parameters recommended by IPEM and NessAiver (see Table 1) and a delayed reconstruction. Acquisitions used the same bandwidth (BW) on each scanner regardless of method, such that the only sequence parameters which varied between the acquisitions were the TE, TR and SW. For both the IPEM and NessAiver sequences "dynamic" acquisitions were performed; producing two sets of images with five seconds between acquisitions. This was specified to prevent image pixel scaling affecting subtraction calculations between sequential images. Multiple repeats were acquired for each sequence, using a protocol that alternated between the IPEM and NessAiver recommended sequences.

Images were acquired on two scanners, in two different receive coil arrangements, in order to simulate naturally "high"(er) and "low"(er) SNR setups:

- **High SNR** - 3.0 T Philips Elition X with a dS HeadNeck 3.0T coil loaded as for manufacturer QC (Fig. b). In total 38 acquisitions of each sequence were performed, with the coil unloaded and reloaded 10 times across these repeats.
- **Low SNR** - 1.5 T Siemens Avanto Fit with no peripheral coils and the integrated body coil loaded as for manufacturer QC (Fig. a). In total 48 acquisitions of each sequence were performed, with the coil unloaded and reloaded 5 times across these repeats.

Coil arrangements were chosen such that transverse images of the phantoms in each arrangement were the same shape and had similar proportions of phantom and background ROI areas.

SNR was calculated for all sets of images, via the three methods outlined in section 1.2, using both the IPEM and NessAiver recommended ROIs. As such, for each dynamic acquisition, 10 SNR results are calculated for each individual element image pair (see Table 2).

A program (*SNR_stab_analysis*) was written in Python 3.8[14], to semi-automate the calculation of SNR values via each method. A flowchart of the code's function can be seen in Fig. 3. CE images are generated using a sum of squares (SoS) combination of the individual images. The NessAiver recommended ROIs were produced using the skimage[15] watershed algorithm. The user is asked to visually confirm that the phantom mask accurately delineates the periphery of the phantom. Then, in order to avoid image artefacts around the periphery

Table 2
SNR results produced from each dynamic acquisition (two images).

Result Description	ROIs	Calculation	SNR Results per Dynamic Acquisition
SNR_{sub} *IPEM ROIs*	IPEM (Fig. 1a)	eqn. 2	1
SNR_{sub} NessAiver ROIs	NessAiver (Fig. 1b)	eqn. 2	1
$SNR_{B\sigma}$ IPEM ROIs	IPEM (Fig. 1a)	eqn. 3	2
$SNR_{B\sigma}$ NessAiver ROIs	NessAiver (Fig. 1b)	eqn. 3	2
$SNR_{B\mu}$ IPEM ROIs	IPEM (Fig. 1a)	eqn. 4	2
$SNR_{B\mu}$ NessAiver ROIs	NessAiver (Fig. 1b)	eqn. 4	2

of the phantom, the phantom ROI (A in Fig. 1b) is generated by contracting the phantom mask by 4 pixels and the air ROI (B in Fig. 1b) is generated by expanding the phantom mask by 5 pixels and inverting it. This is the same method for generating the ROIs as recommended in NessAiver's report[8]. Standardisation in the selection of ROIs using masking thresholds, should reduce errors due to incorrect positioning and eliminate the need for manual intervention (thereby reducing operator burden)[16].

In contrast to the NessAiver method, the IPEM recommended ROIs are of fixed size: The size of the phantom ROI (A in Fig. 1a) corresponds to 75% of the phantom area in the image, matching the NEMA specification[4]. Meanwhile, the air ROIs (B in Fig. 1a) have a radius equal to 1/12 of the matrix dimensions, with the aim to reproduce the single image ROI placement in IPEM Report 112 Fig. 3.3[7]. The air ROIs are defined in fixed locations, and the location of the phantom ROI is based on the centre of mass of the generated phantom mask. *SNR_stab_analysis* then performs the calculations in Table 2, before outputting the results to Excel.

In order to compare the variability in SNR results across different evaluation methods and coil elements, SNR results were normalised by dividing them by the average SNR result across all repeats for the evaluation method. The SD of the normalised SNR results was then calculated for each set of repeats, with the normalised standard deviation offering a measure of the variability in the SNR results.

For each SNR result, the percentage deviation from the mean SNR result for each set of repeats was also calculated. An F-Test was then performed on this data, in order to establish the significance level to which it could be said that the variance in normalised SNR calculated through one method is greater than another.

In order to simulate a reduction in SNR, identical sequences to those in Table 1 were acquired with the SW reduced by ~10%: 4.5 mm for the IPEM sequence and 1.1 mm for the NessAiver sequence. Five acquisitions of each sequence were acquired on both scanner setups and SNR calculated through each method. Using a single tailed Welch's t-test, the results from the reduced SW acquisitions were then compared to the standard acquisitions; in order to determine the significance level to which each method was able to detect a reduction in SNR.

3. Results

Tables 3 to 6 report the SD in the normalised SNR results for each combination of calculation method, ROI type, and sequence, for CE and IE images, from the 3.0 T and 1.5 T scanners. Standard deviations are reported as a percentage of the mean SNR across all repeats.

Fig. 4 depicts the variability in SNR results across all coil elements comparing three methods of measuring SNR: Using the *IPEM Recommended Method*. Using the NessAiver recommended sequence and ROIs, and the $SNR_{B\sigma}$ calculation (*NessAiver Noise-SD Method*). And using the NessAiver recommended sequence and ROIs, and the $SNR_{B\mu}$ calculation (*NessAiver Noise-Average Method*).

Tables 7 to 10 report the single tailed F-test[17] results for equality

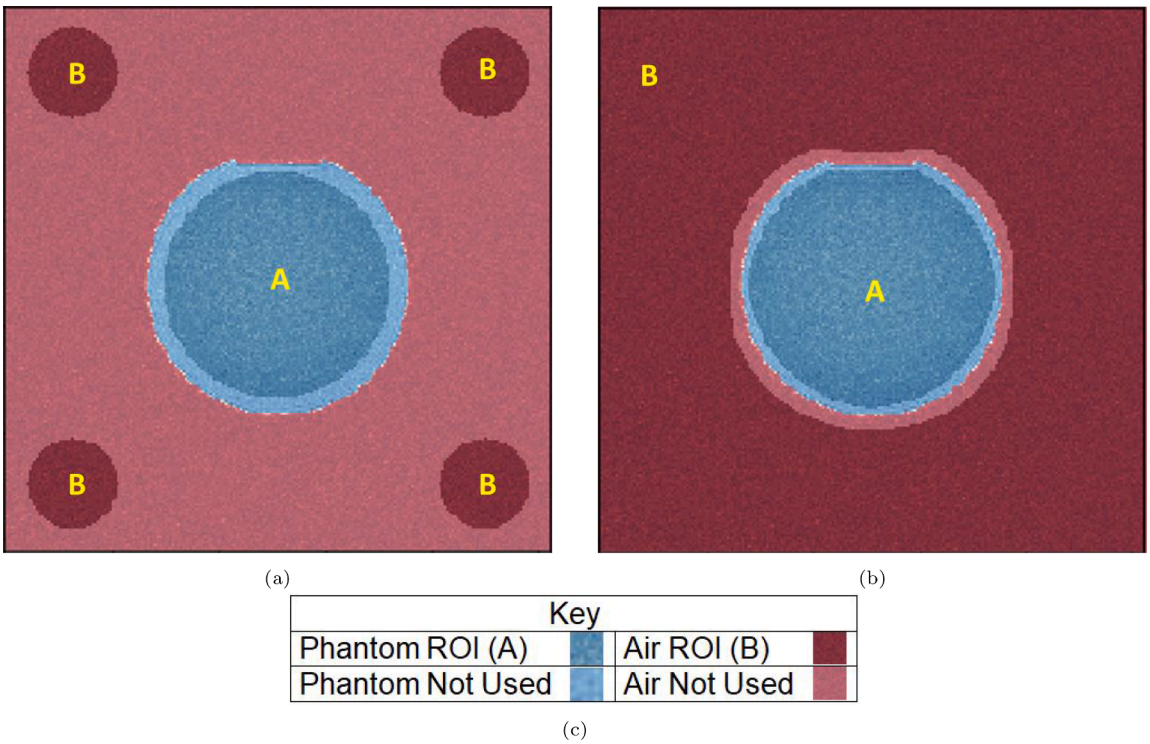

Fig. 1. Regions of interest used for SNR calculation ROIs recommended by (a) IPEM[7,9] and (b) NessAiver[8]. A defines the "phantom ROI" and B defines the "air ROI". The Key (c) is the same for both (a) and (b). The phantom ROI in (a) should cover 75% of the image of the signal-producing volume of the phantom[4]. For subtraction calculations, only the phantom ROI (A) is used from each method (a) and (b).

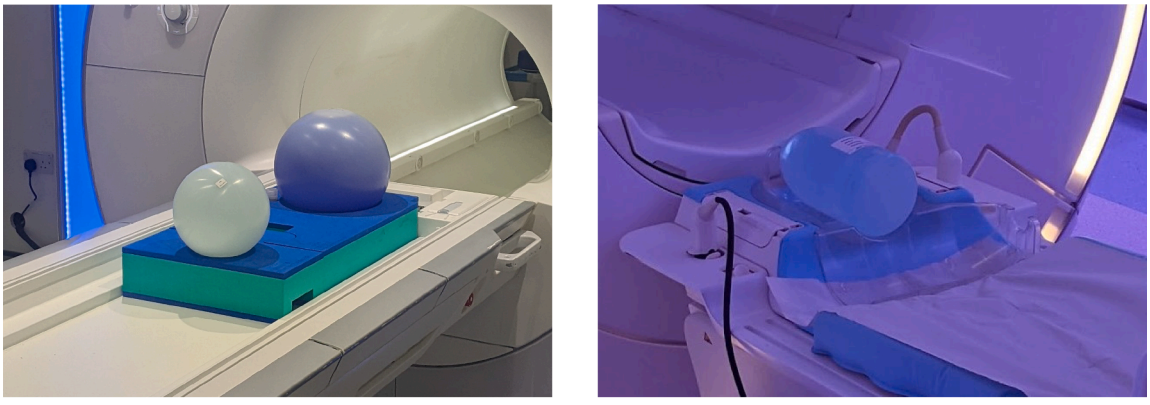

Fig. 2. Loading strategies used to simulate naturally "low"(er) and "high"(er) SNR setups: (a) Low SNR, no peripheral coils and the integrated body coil loaded as for manufacturer QC using three phantoms (Kugel D240, Kugel D165, and Philips Phantom Plastic Bottle-2) in the assigned holder (pictured away from isocentre), and (b) high SNR, dS HeadNeck 3.0T coil loaded as for manufacturer QC using a 3000cc phantom bottle containing Spectrasyn 4[13] in the assigned holder (pictured without top of coil, and away from isocentre).

of two variances, when comparing three methods of SNR measurement: Using the IPEM Recommended method. Using the NessAiver recommended sequence and ROIs, and the $SNR_{B\sigma}$ calculation (*NessAiver Noise-SD Method*). And using the NessAiver recommended sequence and ROIs, and the $SNR_{B\mu}$ calculation (*NessAiver Noise-Average Method*).

Tables 11 and 12 report the single tailed Welch's t-test results assessing each method's ability to detect a reduction in SNR.

4. Discussion

4.1. Limitations

Evaluations of IE images from elements away from isocentre, towards the neck on the HeadNeck coil arrangement on the 3.0 T, resulted in a higher SD than expected for routine examination. This is believed to be as a result of the very low signal present in the images, which may be a consequence of the receiving coil being far from the excited slice.. Typically, for routine examination of Head and Head/Neck coils (and other long coils), the department scrutinises coronal images, which puts the excited slice close to as many coil elements as possible, including the peripheral elements. Furthermore, where no single plane adequately samples all coil elements, NessAiver also recommends that additional acquisitions should take place across multiple planes as necessary[8]. However, for the purpose of this investigation, transverse images were acquired on the HeadNeck coil at isocentre in order to produce similar images from the 1.5 T and 3.0 T arrangements.

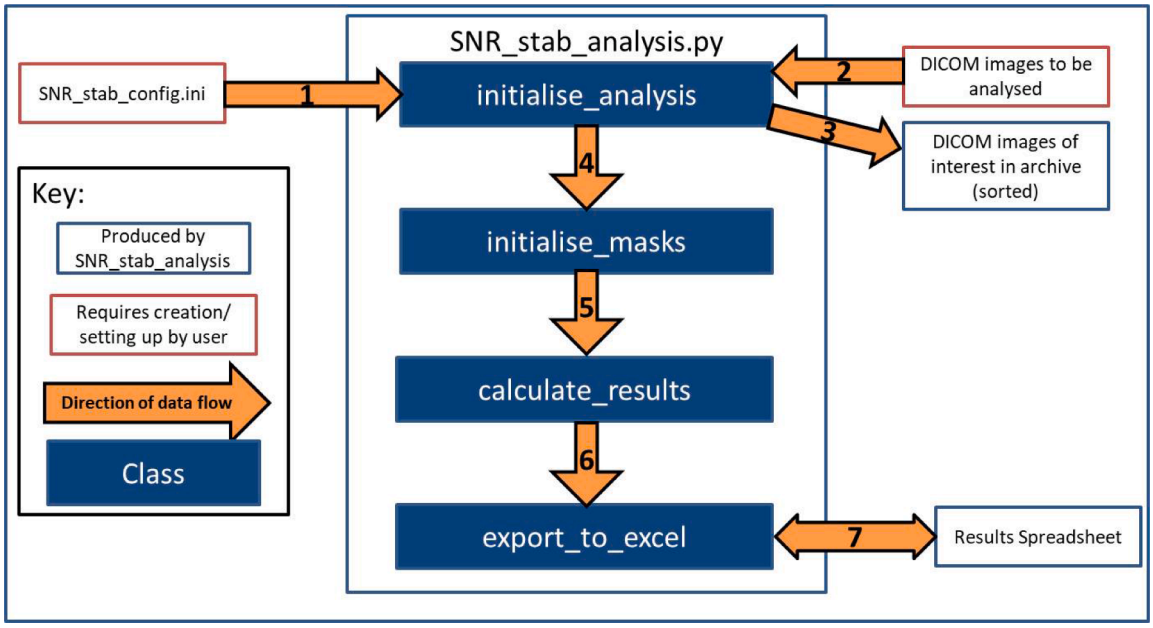

Fig. 3. *SNR_stab_analysis* architecture.

Table 3
SD in normalised SNR through different calculation methods for CE images from the 1.5 T scanner. The *IPEM Recommended Method* is highlighted in bold.

Sequence	ROI	SD (%)		
		SNR_{Sub} (Eqn. 2)	$SNR_{B\sigma}$ (Eqn. 3)	$SNR_{B\mu}$ (Eqn. 4)
IPEM (Table 1a)	IPEM (Fig. 1a)	**4.94**	6.39	1.00
IPEM (Table 1a)	NessAiver (Fig. 1b)	4.98	6.05	0.971
NessAiver (Table 1b)	IPEM (Fig. 1a)	3.77	5.56	1.04
NessAiver (Table 1b)	NessAiver (Fig. 1b)	3.65	5.48	1.05

Table 4
SD in normalised SNR through different calculation methods for CE images from the 3.0 T scanner. The *IPEM Recommended Method* is highlighted in bold.

Sequence	ROI	SD (%)		
		SNR_{Sub} (Eqn. 2)	$SNR_{B\sigma}$ (Eqn. 3)	$SNR_{B\mu}$ (Eqn. 4)
IPEM (Table 1a)	IPEM (Fig. 1a)	**7.33**	1.47	0.551
IPEM (Table 1a)	NessAiver (Fig. 1b)	8.28	5.46	2.65
NessAiver (Table 1b)	IPEM (Fig. 1a)	1.24	1.03	0.849
NessAiver (Table 1b)	NessAiver (Fig. 1b)	1.20	0.709	0.718

Table 5
SD in normalised SNR through different calculation methods for IE images from the 1.5 T scanner. The *IPEM Recommended Method* is highlighted in bold.

Sequence	ROI	SD (%)		
		SNR_{Sub} (Eqn. 2)	$SNR_{B\sigma}$ (Eqn. 3)	$SNR_{B\mu}$ (Eqn. 4)
IPEM (Table 1a)	IPEM (Fig. 1a)	**16.7**	14.9	6.89
IPEM (Table 1a)	NessAiver (Fig. 1b)	16.7	14.0	6.69
NessAiver (Table 1b)	IPEM (Fig. 1a)	14.2	13.6	5.26
NessAiver (Table 1b)	NessAiver (Fig. 1b)	14.1	13.1	5.22

In addition, on two occasions, Philips's SmartSelect system had determined that a different range of elements (to normal) should be sampled for the specified image sequence. Specifically, this affected the ordering of individual coil element images. As such, to ensure the comparison of the consistency of measurements from elements was valid, the affected images were removed from the dataset. In total two acquisitions were affected, corresponding to four images in total (two using the IPEM recommended sequence and two using the NessAiver recommended sequence).

Table 6
SD in normalised SNR through different calculation methods for IE images from the 3.0 T scanner. The *IPEM Recommended Method* is highlighted in bold.

Sequence	ROI	SD (%)		
		SNR_{Sub} (Eqn. 2)	$SNR_{B\sigma}$ (Eqn. 3)	$SNR_{B\mu}$ (Eqn. 4)
IPEM (Table 1a)	IPEM (Fig. 1a)	**7.29**	6.80	6.96
IPEM (Table 1a)	NessAiver (Fig. 1b)	7.25	7.12	8.16
NessAiver (Table 1b)	IPEM (Fig. 1a)	4.72	5.76	5.88
NessAiver (Table 1b)	NessAiver (Fig. 1b)	4.47	5.44	5.47

It is also acknowledged that the method used to simulate a reduction in SNR was not representative of a situation where there is a fault in individual receive channels. Additional study may be necessary, using simulated or genuine faulty channel images, to understand the extent to which the methods are able to detect faults in reconstructed CE images. Nevertheless, it can be assumed that quantitative or qualitative analysis of individual channel images using either method would be sufficient to detect receive channel failures.

Finally, it is recognised that the study has a sample size limited to two models of scanner.

4.2. Comparing Analysis Methods

Calculation of SNR through Equations 2,3 and 4 did not produce identical values. Additionally, images acquired with the sequence parameters recommended by IPEM (Table 1a) produced images with a higher SNR than those acquired with sequence parameters recommended by NessAiver (Table 1b). To allow for comparison, SNR values were normalised across each ret of repeats.

Setting aside the rationale for a low SNR image in the case of NessAiver in Section 1.3, when analysing images of phantoms, the value of SNR is a largely arbitrary quantitative metric by itself; what truly matters is the ability to detect a change in performance. As such, lower SNR

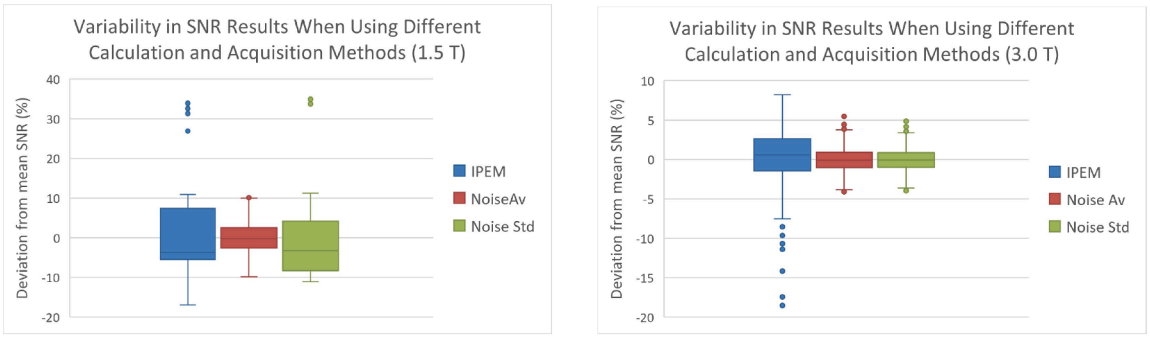

Fig. 4. Box and Whisker plots depicting variability in SNR results across all coil elements in the (a) "low"(er) and (b) "high"(er) SNR setups. Three methods of measuring SNR are compared: **IPEM** - IPEM Recommended Method: Seq. Table 1(a), ROIs. Fig. 1a, Eqn. 2, n=24 **Noise Av** - NessAiver Noise-Average Method: Seq. Table 1(b), ROIs. Fig. 1b, Eqn. 3, n=48 **Noise Std** - NessAiver Noise-SD Method: Seq. Table 1(b), ROIs. Fig. 1b, Eqn. 4, n=48.

Table 7
F-test assessing the significance level to which the variance in normalised SNR is greater for "SNR Evaluation Method 1" than "SNR Evaluation Method 2" for CE images from the 1.5 T scanner. IPEM Recommended Method: Seq. Table 1(a), ROIs. Fig. 1a, Eqn. 2, n=24 NessAiver Noise-SD Method: Seq. Table 1(b), ROIs. Fig. 1b, Eqn. 3, n=48 NessAiver Noise-Average Method: Seq. Table 1(b), ROIs. Fig. 1b, Eqn. 4, n=48.

SNR Evaluation Method 1	SNR Evaluation Method 2	F-test	
		F	p
IPEM Recommended Method	NessAiver Noise-SD Method	0.81	0.70
IPEM Recommended Method	NessAiver Noise-Average Method	22	<0.001
NessAiver Noise-SD Method	NessAiver Noise-Average Method	27	<0.001

Table 8
F-test assessing the significance level to which the variance in normalised SNR is greater for "SNR Evaluation Method 1" than "SNR Evaluation Method 2" for CE images from the 3.0 T scanner. IPEM Recommended Method: Seq. Table 1(a), ROIs. Fig. 1a, Eqn. 2, n=19 NessAiver Noise-SD Method: Seq. Table 1(b), ROIs. Fig. 1b, Eqn. 3, n=38 NessAiver Noise-Average Method: Seq. Table 1(b), ROIs. Fig. 1b, Eqn. 4, n=38.

SNR Evaluation Method 1	SNR Evaluation Method 2	F-test	
		F	p
IPEM Recommended Method	NessAiver Noise-SD Method	107	<0.001
IPEM Recommended Method	NessAiver Noise-Average Method	104	<0.001
NessAiver Noise-SD Method	NessAiver Noise-Average Method	0.98	0.53

Table 9
F-test assessing the significance level to which the variance in normalised SNR is greater for "SNR Evaluation Method 1" than "SNR Evaluation Method 2" for IE images from the 1.5 T scanner. IPEM Recommended Method: Seq. Table 1(a), ROIs. Fig. 1a, Eqn. 2, n=48 NessAiver Noise-SD Method: Seq. Table 1(b), ROIs. Fig. 1b, Eqn. 3, n=96 NessAiver Noise-Average Method: Seq. Table 1(b), ROIs. Fig. 1b, Eqn. 4, n=96.

SNR Evaluation Method 1	SNR Evaluation Method 2	F-test	
		F	p
IPEM Recommended Method	NessAiver Noise-SD Method	1.6	0.23
IPEM Recommended Method	NessAiver Noise-Average Method	10	<0.001
NessAiver Noise-SD Method	NessAiver Noise-Average Method	6.3	<0.001

Table 10
F-test assessing the significance level to which the variance in normalised SNR is greater for "SNR Evaluation Method 1" than "SNR Evaluation Method 2" for IE images from the 3.0 T scanner. IPEM Recommended Method: Seq. Table 1(a), ROIs. Fig. 1a, Eqn. 2, n=304 NessAiver Noise-SD Method: Seq. Table 1(b), ROIs. Fig. 1b, Eqn. 3, n=608 NessAiver Noise-Average Method: Seq. Table 1(b), ROIs. Fig. 1b, Eqn. 4, n=608.

SNR Evaluation Method 1	SNR Evaluation Method 2	F-test	
		F	p
IPEM Recommended Method	NessAiver Noise-SD Method	1.8	<0.001
IPEM Recommended Method	NessAiver Noise-Average Method	1.8	<0.001
NessAiver Noise-SD Method	NessAiver Noise-Average Method	0.99	0.55

Table 11
Single tailed Welch's t-tests, assessing the significance level to which it can be said that the reduced SW acquisition on the 1.5 T scanner produces lower CE SNR results. IPEM Recommended Method: Seq. Table 1(a), ROIs. Fig. 1a, Eqn. 2 NessAiver Noise-SD Method: Seq. Table 1(b), ROIs. Fig. 1b, Eqn. 3 NessAiver Noise-Average Method: Seq. Table 1(b), ROIs. Fig. 1b, Eqn. 4.

SNR Evaluation Method	Standard SW		Reduced SW		Welch's t-test	
	M	SD	M	SD	t (DF)	p
IPEM Recommended Method	176	8.71	159	8.43	4.14 (5.9)	0.0031
NessAiver Noise-SD Method	38.7	2.14	37.1	2.23	1.57 (11)	0.073
NessAiver Noise-Average Method	39.3	0.418	36.2	0.335	19.6 (12)	<0.001

Table 12
Single tailed Welch's t-tests, assessing the significance level to which it can be said that the reduced SW acquisition on the 3.0 T scanner produces lower CE SNR results. IPEM Recommended Method: Seq. Table 1(a), ROIs. Fig. 1a, Eqn. 2 NessAiver Noise-SD Method: Seq. Table 1(b), ROIs. Fig. 1b, Eqn. 3 NessAiver Noise-Average Method: Seq. Table 1(b), ROIs. Fig. 1b, Eqn. 4.

SNR Evaluation Method	Standard SW		Reduced SW		Welch's t-test	
	M	SD	M	SD	t (DF)	p
IPEM Recommended Method	236	17.3	233	12.3	1.91 (8.7)	0.045
NessAiver Noise-SD Method	47.4	0.340	46.3	0.164	14.4 (31)	<0.001
NessAiver Noise-Average Method	107	0.760	102	0.306	32.1 (38)	<0.001

images should not be a problem when the SNR is being used as a quality control monitor, but should be borne in mind if the SNR is being compared against values obtained by other means[18]. For this reason, the normalised SD results provide a useful metric: A more repeatable measure of assessing SNR means that smaller discrepancies can be attributed to equipment performance rather than user error, and tighter action levels can be defined for investigation and rectification.

The *IPEM Recommended Method* requires the longest scan time and is laborious to perform. Moreover, as the method requires comparison between two phantom images, the potential movement of phantom contents between acquisitions will introduce unintended variability. To mitigate this, further time allowances may be required to allow contents to settle. This concern is not relevant to methods which rely on the analysis of single images. Since the NEMA subtraction method requires assessment of a "regularly shaped geometric area"[4], the process of automatic ROI generation using contracted phantom masks is not suitable for irregularly shaped phantom images (such as sagittal images of the foot phantom). As such, when using this method, phantom and air ROIs need to be defined for each phantom setup, and small variations in phantom positioning could have a significant effect on the SNR results; especially if the ROIs are defined in fixed locations. A more efficient method would be to switch to the *NessAiver Noise-Average Method* or *NessAiver Noise-SD Method* where ROIs don't need to be explicitly defined for every coil setup because the ROIs can be generated semi-automatically (using a watershed algorithm).

Additionally, either method would only require one image per SNR result, and when combined with time-saved in the NessAiver sequence, the methods would provide a 90% overall reduction in sequence duration: Acquisition time for the IPEM sequence (Table 1a) is five times greater than for the NessAiver recommended sequence (Table 1b), and since the subtraction method requires two image repeats per calculation, acquisition time increases by a further factor of two.

Looking at Tables 3 to 6, assessment of SNR using the *NessAiver Noise-Average Method* (Equation 4) typically offered the lowest variability in SNR results. The method performed consistently well for CE and IE images on both the 1.5 T and 3.0 T scanner.

Comparing the *IPEM Recommended Method* to the *NessAiver Noise-SD Method*: In all situations, except the CE assessment on the 1.5 T, the *IPEM Recommended Method* provided greater variability in SNR results than the *NessAiver Noise-SD Method* ($p \leq 0.023$). For the CE assessment on the 1.5 T, the difference in SD between the two evaluation methods was small (Table 3) and not significant $p \leq 0.05$ ($P = 0.70$). The results suggest that moving from the *IPEM Recommended Method* to the *NessAiver Noise-SD Method* will result in more repeatable SNR results.

Comparing the *IPEM Recommended Method* to the *NessAiver Noise-Average Method*: In all situations, the *IPEM Recommended Method* provided greater variability in SNR results than the *NessAiver Noise-Average Method* ($p < 0.001$). This suggests that moving from the *IPEM Recommended Method* to the *NessAiver Noise-Average Method* will also result in more repeatable SNR results.

Comparing the *NessAiver Noise-SD Method* and the *NessAiver Noise-Average Method*: The *NessAiver Noise-SD Method* provided greater variability in SNR results than the *NessAiver Noise-Average Method* for both CE and IE images on the 1.5 T ($p < 0.001$). However, on the 3.0 T, the two techniques performed similarly, with little change in SD for both IE and CE images (Tables 4 and 6) where the *NessAiver Noise-Average Method* provided greater variability in SNR results, but not to a significant extent ($p \geq 0.53$). This suggests that in the majority of situations calculating SNR using the *NessAiver Noise-Average Method* will result in more repeatable SNR results than using the *NessAiver Noise-SD Method*.

These results are in general agreement with a similar deviation comparison completed by NessAiver[8].

Looking at tables 11 and 12, both the *IPEM Recommended Method*, and the *NessAiver Noise-Average Method* were able to detect a simulated reduction in SNR with $p < 0.05$. However, the significance level to which a simulated reduction in SNR could be detected using the *IPEM Recommended Method* was less. It is also worth noting that the simulated reduction in SNR is theoretically less with the NessAiver sequence than the IPEM sequence. The IPEM sequence SW was reduced by 10% and the NessAiver sequence SW by 8.3%.

5. Conclusion

Of the SNR evaluation methods tested, this study suggests that calculating SNR using the *NessAiver Noise-Average Method*, provided the most repeatable measure of SNR. The *NessAiver Noise-Average Method* was significantly more repeatable and better able to detect a reduction in SNR than the *IPEM Recommended Method*. Furthermore, using the *NessAiver Noise-Average Method* results in a reduction in acquisition time of 90%, when compared to the *IPEM Recommended Method*.

This study suggests that using the *NessAiver Noise-Average Method* is a more optimal method of assessing assessing SNR in phantoms for routine QA than the current *IPEM Recommended Method*[3].

Funding

None.

Ethical approval

Not required.

Acknowledgements

Competing interests: None declared.

References

[1] Siemens, Head/Neck 64 Coil Description (accessed 20/06/2022), https://www.siemens-healthineers.com/en-uk/magnetic-resonance-imaging/options-and-upgrades/coils/64-channel-head-neck-coil.
[2] S. Bacon, D. Wilson, Issues affecting the performance testing of modern MRI scanners. 2014 Conference Abstracts Vol II: October - December, IPEM, 2014, p. 46.
[3] A. Barnes, G. Charles-Edwards, G. Coutts, P. Gatehouse, M. Graves, K. Lymer, I. Marshall, A. McCann, D. McRobbie, S. Nicholas, A. Papadaki, A. Patterson, S. Semple, J. Thornton, N. Weir, D. Wilson, S. Withey, G. Wright, IPEM Report 112: Quality Control and Artefacts in Magnetic Resonance Imaging. Technical Report, IPEM112, 2017.
[4] NEMA, NEMA Standards Publication MS 1-2008: Determination of Signal-to-Noise Ratio (SNR) in Diagnostic Magnetic Resonance Imaging, Rosslyn, Va: National Electrical... 2008 (2021) 1–21.
[5] L. Kaufman, D.M. Kramer, L.E. Crooks, D.A. Ortendahl, Measuring signal-to-noise ratios in MR imaging, Radiology (1989), https://doi.org/10.1148/radiology.173.1.2781018.
[6] C.D. Constantinides, E. Atalar, E.R. McVeigh, Signal-to-noise measurements in magnitude images from NMR phased arrays, 1997, /pmc/articles/PMC2570034/pmc/articles/PMC2570034/?report=abstract https://www.ncbi.nlm.nih.gov/pmc/articles/PMC2570034. 10.1002/mrm.1910380524.
[7] A. Barnes, G. Charles-Edwards, G. Coutts, P. Gatehouse, M. Graves, K. Lymer, I. Marshall, A. McCann, D. McRobbie, S. Nicholas, A. Papadaki, A. Patterson, S. Semple, J. Thornton, N. Weir, D. Wilson, S. Withey, G. Wright, Fig. 3.3. Quality Control and Artefacts in Magnetic Resonance Imaging, IPEM, 2017, p. 24.
[8] M. NessAiver, A Complete MRI Physics Services Provider RF Coil Testing-The Simply Physics way (accessed 20/06/2022). Technical Report, 2019.http://www.amos3.aapm.org/abstracts/pdf/146-47286-486612-152730-1165741637.pdf.
[9] A. Barnes, G. Charles-Edwards, G. Coutts, P. Gatehouse, M. Graves, K. Lymer, I. Marshall, A. McCann, D. McRobbie, S. Nicholas, A. Papadaki, A. Patterson, S. Semple, J. Thornton, N. Weir, D. Wilson, S. Withey, G. Wright, Figure 3.2. Quality Control and Artefacts in Magnetic Resonance Imaging, IPEM, 2017, p. 23.
[10] C.G. Koay, P.J. Basser, Analytically exact correction scheme for signal extraction from noisy magnitude MR signals, Journal of Magnetic Resonance 179 (2) (2006) 317–322, https://doi.org/10.1016/j.jmr.2006.01.016.
[11] O. Dietrich, J.G. Raya, S.B. Reeder, M. Ingrisch, M.F. Reiser, S.O. Schoenberg, Influence of multichannel combination, parallel imaging and other reconstruction techniques on MRI noise characteristics, Magnetic Resonance Imaging 26 (6) (2008) 754–762, https://doi.org/10.1016/j.mri.2008.02.001.
[12] D.O. Walsh, A.F. Gmitro, M.W. Marcellin, Adaptive reconstruction of phased array MR imagery, Magnetic Resonance in Medicine (2000), https://doi.org/10.1002/(SICI)1522-2594(200005)43:5<682::AID-MRM10>3.0.CO;2-G.
[13] ExxonMobil, Datasheet - ExxonMobil SpectraSyn 4. Technical Report, 2019.https://www.exxonmobilchemical.com/ContactUs

[14] The Python Language Reference Python 3.8.13 documentation - Reference Document (accessed 20/06/2022)https://www.docs.python.org/3.8/reference/index.htmlreference-index.
[15] Module: segmentation skimage v0.19.2 Module Description (accessed 20/06/2022), https://www.scikit-image.org/docs/stable/api/skimage.segmentation.html?highlight=watershedskimage.segmentation.watershed.
[16] A.J. McCann, A. Workman, C. McGrath, A quick and robust method for measurement of signal-to-noise ratio in MRI, Physics in Medicine and Biology 58 (11) (2013) 3775–3790, https://doi.org/10.1088/0031-9155/58/11/3775.
[17] G.W. Snedecor, W.G. Cochran, Statistical methods, 8thedn, Ames: Iowa State Univ. Press Iowa 54 (1989) 71–82.
[18] M.J. Firbank, A. Coulthard, R.M. Harrison, E.D. Williams, A comparison of two methods for measuring the signal to noise ratio on MR images, Physics in Medicine and Biology 44 (12) (1999) 261–264, https://doi.org/10.1088/0031-9155/44/12/403.